Transmission Line above Ground: Circuit Models for the Open, Short, and Ground Rod Terminating Loads

Larry K. Warne[1,*], Salvatore Campione[1], and Rebecca S. Coats[1]

[1]Sandia National Laboratories, P.O. Box 5800, Albuquerque, NM, USA

*corresponding author, E-mail: lkwarne@sandia.gov

Abstract

In this paper we investigate a transmission line consisting of an aerial wire above a conducting ground excited by a plane wave. In particular, we are interested in constructing simple circuit models for the terminating impedances at the ends of the line including radiation effects. We consider the following load topologies: open circuit, short circuit, and grounded rods. Results from the transmission line model with these loads show good agreement with full-wave simulations. These circuit models can be then used to achieve fast and reliable results in a timely manner, as opposed to the generally slow response of full-wave simulators, especially for long lines.

1. Introduction

In this paper we investigate transmission line models for an aerial wire above a conductive half space. Many contributions have modeled such situations [1-9] and have provided powerful formulas for the ground impedance and admittance for aerial and buried conductors, as well as multiple-wire modes and high-frequency modes [5, 10-13]. Here, however, we concentrate on developing lumped loads representing corrections to the distributed transmission line elements in order to approximately account for the fringe field corrections at the ends of the line under open circuit and short circuit terminations and grounded rods, as well as elements to account for radiation of the line. Derivations of formulas discussed in this paper can be found in [14], where we also discuss and compare the two existing approaches for modeling plane wave field coupling to transmission lines in order to sort out the relevant sources and the associated meaning of the voltage and current solutions. The different bases for the current decomposition (for example, transmission line and antenna modes) are also discussed in [14], and are not reported here for brevity.

For an open circuit termination, since the distributed admittances of the transmission line model for dense lower dielectric half spaces are typically dominated by the air region above the conductive half space (in other words, the ground admittance has negligible effects for aerial lines [13]), the lumped load capacitance and air conductance elements will have reasonably broad applicability. We include an additional term here in the load capacitance [15].

For a short circuit termination, since we will use an image in the ground to describe the return current, the lumped inductance element will be somewhat approximate (but yet useful) unless the skin depth in the conductive half space becomes smaller than the line height above the ground.

The lumped load for a grounded rod will be generated through a transmission line implementation to model arbitrary length rods [16]. The approach taken here is to introduce an end load which restores the low frequency limit. In this way, if the end is not visible due to decay we do not see the end load.

Furthermore, the radiation elements are derived for a line with a reasonably concentrated image current, and are thus also limited to this small skin depth case. We note that for the large skin depth case, we expect the ground losses to dominate over the radiation losses, and furthermore, the damping may spread out resonant behavior in frequency to the point where the exact spectral position is less important. We also briefly refer to the alternative approach of using the Wiener-Hopf reflection coefficient to treat both long lines and larger skin depths when the lines end in an open circuit.

Our main contribution is to compare results from the analytical model to full wave simulations (using either EIGER [16, 17], a Sandia National Laboratories method-of-moments code, or CST Microwave Studio [18]) for the cases of open-open, short-short, and open-short terminations, as well as grounded rods. Our work provides a verification of the circuit models for various loads through full wave simulations. We believe this analytical method is an alternative, fast and reliable option to a full-wave solution, which could be rather slow when considering long lines.

2. Transmission line model

Figure 1 shows an example of a transmission line above ground with "open" (panel (a)), "short" (panel (b)), and “ground rods” (panel (c)) circuit loads at both ends.

We employ a one-dimensional transmission line model

for the coupling to a wire above a finitely conducting ground [19-22], where the transverse dimension is modeled in terms of cross sectional per unit length circuit parameters [1-4, 8, 9]. The time dependence $\exp(-i\omega t)$ is implicitly assumed here. Note these references do not discuss the terminating loads circuit models capturing the local three-dimensional field, subject of this work. The voltage equation and current equations are

$$\frac{dV}{dz} = E^{oc} - ZI, \qquad \frac{dI}{dz} = -YV, \tag{1}$$

where the impedance per unit length is $Z = Z_w - i\omega L_e + Z_4$, with external inductance per unit length $L_e = L_2 + L_0$, where the wire dielectric coating inductance per unit length is $L_2 = \mu_0 \ln(b/a)/(2\pi)$ and the air inductance per unit length is $L_0 = \mu_0 \operatorname{arccosh}(h/b)/(2\pi)$. The impedance per unit length of the wire at high frequencies is $Z_w \sim Z_s/(2\pi a)$ where the surface impedance of the metal is $Z_s = (1-i)R_s$, the surface resistance is $R_s = 1/(\sigma\delta)$, with the skin depth $\delta = \sqrt{2/(\omega\mu)}$, and μ and σ are the metal permeability and conductivity, respectively. The admittance per unit length is $1/Y = 1/Y_e + 1/Y_4$, where the external admittance per unit length is $1/Y_e = 1/(G_0 - i\omega C_0) + 1/(i\omega C_2)$, the wire dielectric coating capacitance per unit length is $C_2 = 2\pi\varepsilon_w/\ln(b/a)$, and the air capacitance per unit length and conductance per unit length $C_0 + iG_0/\omega = 2\pi\varepsilon_w/\operatorname{arccosh}(h/b)$, with $\varepsilon_w = \varepsilon_w' + i\sigma_w/\omega$ the complex permittivity of air, μ_0 the permeability of free space, b the coating radius, a the wire radius, and h the wire height with respect to ground. The ground parameters for $h > b$ are taken as $Z_4 \approx -i\omega\mu_0 h H_0^{(1)}(k_4 h)/\left[2\, k_4 h H_1^{(1)}(k_4 h)\right]$ and $Y_4 \approx -i\pi(\omega\varepsilon_4 - i\sigma_4) k_4 h H_1^{(1)}(k_4 h)/H_0^{(1)}(k_4 h)$ with ground propagation constant $k_4 = \sqrt{\omega\mu_0(\omega\varepsilon_4 + i\sigma_4)}$, ε_4 the ground permittivity, and σ_4 the ground conductivity. The value of Y_4 in [2, 8, 9, 23] is appropriate for wires near the ground or buried below the ground. However, we have found that Y_4 plays a negligible role in aerial lines [13] (which is consistent with the broad applicability of the terminating load capacitance). The external source term for plane wave incidence at oblique angle θ_0 with respect to z is $E^{oc}(z) = E_0^{oc} e^{ikz\cos\theta_0}$ where $k = \omega\sqrt{\mu_0 \varepsilon_w}$.

In this paper we consider the case where the air conductivity is small enough that we can treat it as a damping effect along the transmission line, but not so large that it causes the air skin depth to become comparable to, or less than, the height of the transmission line above the ground. If the air conductivity is large, the terminating load effects discussed here are likely not important due to the large line losses, and the fact that the line is significantly changed from the case where it is interacting with the ground.

(a) Open-circuited wire

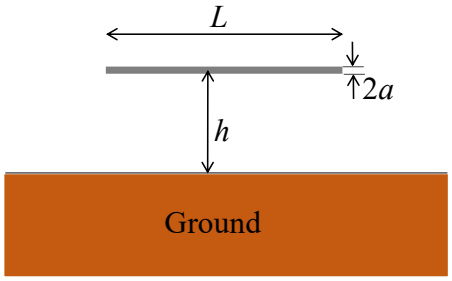

(b) Short-circuited wire

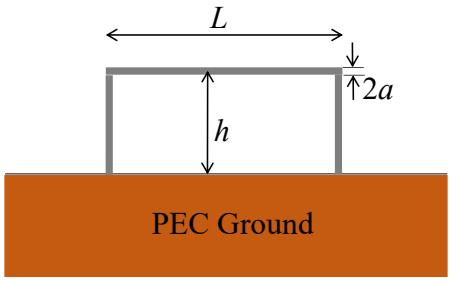

(c) Wire with ground rods

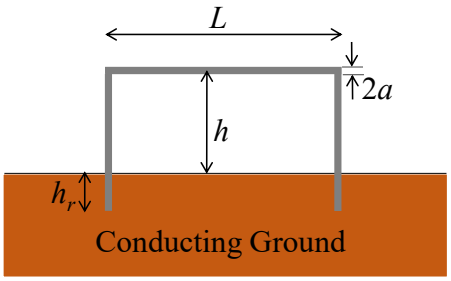

Figure 1: Geometry of a finite wire with length L and radius a above ground for the cases of (a) open-open, (b) short-short, and (c) grounded rods. The down conductors have the same radius as the aerial line.

Elimination of the voltage in the transmission line equations (1) gives

$$\left(\frac{d^2}{dz^2} + k_L^2\right) I = -YE_0^{oc} e^{ikz\cos\theta_0}, \tag{2}$$

where the propagation constant along the line is $k_L = \sqrt{-ZY}$ and the characteristic impedance of the line is $Z_c = \sqrt{Z/Y}$. The general solution can be written as the sum of the particular solution and homogeneous solutions

$$I(z) = I_+ e^{ik_L z} + I_- e^{-ik_L z} + I_p(z), \tag{3}$$

where $I_\pm$ are constants and $I_p(z) = -YE_0^{oc} e^{ikz\cos\theta_0} / \left(k_L^2 - k^2 \cos^2\theta_0\right)$.

The conventional transmission line model uses the electric field component along the line conductors as a drive. To be complete we also require the transverse electric field drive along the transverse load directions at both ends of the line. For a two-wire line along the z axis the distributed sources are a distributed open circuit voltage source equal to the difference between the incident axial drive field at the centroids of current (when driven in a differential mode) in the two conductors (the positive wire reference minus the negative wire reference) $E^{oc} = E_0^{oc} e^{ikz\cos\theta_0} = E_z^{inc}(h_e) - E_z^{inc}(-h_e)$ with $h_e = \sqrt{h^2 - a^2}$. We note that the sign of the distributed voltage source in the transmission line equation means that we are actually imposing a distributed electric field source in the line which opposes the incident field (scattered field). For a finite line over $0 \le z \le \ell$ with a load Z_1 at $z = 0$ and Z_2 at $z = \ell$ we impose the boundary conditions $V(0) = V_0(0) - Z_1 I(0)$ and $V(\ell) = V_0(\ell) + Z_2 I(\ell)$, where the transverse sources are

$$V_0(z) = \int_{C_{h_e}} \underline{E}^{inc} \cdot \underline{dl} = \underline{h}_e \cdot \underline{E}^{inc}, \tag{4}$$

the path C_{h_e} starts on the negative reference conductor (the ground) and proceeds to the positive reference conductor along the center of the load, and the vector $\underline{h}_e$ points from the negative to positive reference conductor along the load. Note again that this end voltage source opposes the incident field (scattered field).

If we consider the case where a ground plane is inserted into the two wire transmission line, the impedance (inductance) per unit length and the characteristic impedance Z_c is cut in half, while the admittance (capacitance) per unit length doubles. The sources E^{oc}, V_0 (and V_t) are left unchanged because the path length is cut in half ($2h_e$ is replaced by h_e), but the reflected plane wave from the surface doubles the tangential magnetic and normal electric drive fields. Thus the voltage is left unchanged but the current doubles.

For a finitely conducting ground half space there will be added contributions to the impedance and to the admittance as well as modifications to the reflected part of the drive fields. Nevertheless, because the line voltage is largely supported by the air region above the ground plane, we expect that in the conventional method the incident (and reflected) transverse voltage must be added to the transmission line voltage to obtain the total voltage. The incident plus reflected plane wave fields (with zero phase reference on the plane interface at $x = 0$) can be written as

$$\begin{aligned} H_y^{inc} + H_y^{ref} &= (E_0/\eta_0)\left(e^{-ikx\sin\theta_0} + R_H e^{ikx\sin\theta_0}\right) e^{ikz\cos\theta_0} \\ E_z^{inc} + E_z^{ref} &= E_0 \sin\theta_0 \left(e^{-ikx\sin\theta_0} - R_H e^{ikx\sin\theta_0}\right) e^{ikz\cos\theta_0} \\ E_x^{inc} + E_x^{ref} &= E_0 \cos\theta_0 \left(e^{-ikx\sin\theta_0} + R_H e^{ikx\sin\theta_0}\right) e^{ikz\cos\theta_0} \end{aligned}, \tag{5}$$

where the TM reflection coefficient is

$$R_H = \frac{(k_4/k)^2 \sin\theta_0 - \sqrt{(k_4/k)^2 - \cos^2\theta_0}}{(k_4/k)^2 \sin\theta_0 + \sqrt{(k_4/k)^2 - \cos^2\theta_0}}, \tag{6}$$

The distributed voltage source in the conventional method is then (note that the fields vanish deep in the ground so the contribution to the source from this region vanishes)

$$\begin{aligned} E^{oc} &= E_0^{oc} e^{ikz\cos\theta_0} = E_z^{inc}(h_e) + E_z^{ref}(h_e) \\ &= E_0 \sin\theta_0 \left(e^{-ikx\sin\theta_0} - R_H e^{ikx\sin\theta_0}\right) e^{ikz\cos\theta_0} = A_0 e^{ikz\cos\theta_0} \end{aligned}, \tag{7}$$

with no distributed short circuit current source, but end transverse sources

$$\begin{aligned} V_0(z) &\approx h_e \left[E_x^{inc}(h_e) + E_x^{ref}(h_e)\right] \\ &\approx 2h_e E_0 \cos\theta_0 \left(e^{-ikx\sin\theta_0} + R_H e^{ikx\sin\theta_0}\right) e^{ikz\cos\theta_0} = V_t^{inc} \end{aligned}, \tag{8}$$

3. Short circuit inductive termination

A simple procedure [15, 24] to find the inductive termination is to use a formula for the static inductance of a rectangular loop [25]. One half this value is differenced by subtraction of the inductance per unit length of a two wire transmission line times the length. This difference forms the estimate for the terminating inductance of the "shorted" end of the resonator

$$L_t \sim 2h \frac{\mu_0}{2\pi} \left[\ln(4h/a) - 2\right] = 2L_t^{GP}, \tag{9}$$

where for the wire above a PEC plane the end load inductance L_t^{GP} is shown in Eq. (9), in which it may be more consistent (and slightly more accurate) to replace h by h_e.

When the down conductor has loss the terminating impedance is $Z_t^{GP} = Z_w h - i\omega L_t^{GP}$. For a finitely conducting half space this will also hold for small skin depth compared to the line height, provided we add a terminating load at the interface, which is discussed in Sec. 6.

4. Open circuit capacitive termination

A similar procedure [24] to find the capacitive termination is to use a formula for the static capacitance of a long or semi-infinite two wire line charged to a potential difference. In this section we take the permittivity of the air ε_w to be real; if it is complex we can either replace ε_w by the real part ε_w' or use the complex permittivity $\varepsilon_w = \varepsilon_w' + i\sigma_w/\omega$ but replace the capacitance C by the combination $C + iG/\omega$; we also ignore the presence of an insulation layer and replace b by a in this section. The iterative procedure is a static version of that used to solve the

problem of a thin cylindrical antenna [26]. The two conductor capacitance per unit length, times the length, is subtracted to yield the terminating capacitance of the "open" end of the resonator. For small a we can write

$$2\pi\varepsilon_w V \sim \Omega q(z) - q(z)\left[\ln\left\{z/(2h)+\sqrt{z^2/(2h)^2+1}\right\} \quad \ln(z/h)\right], \quad (10)$$
$$+\int_0^\infty \left[\frac{1}{|z-z'|}-\frac{1}{\sqrt{4h^2+(z-z')^2}}\right]\left[q(z')-q(z)\right]dz'$$

where we define $\Omega = 2\ln(2h/a)$. An iterative solution is obtained by assuming Ω is large. The leading term is the transmission line capacitance per unit length $C = q_0/V$, where

$$C = \frac{\pi\varepsilon_w}{\operatorname{arccosh}(h/a)} \sim \frac{\pi\varepsilon_w}{\ln(2h/a)} = \frac{2\pi\varepsilon_w}{\Omega}. \quad (11)$$

The next term can be integrated to give the leading terminating capacitance [15]

$$C_t \sim \frac{4\pi h\varepsilon_w}{\Omega^2}. \quad (12)$$

Including the next term yields

$$C_t \sim \frac{2hC}{\Omega}\left(1+4(1-\ln 2)/\Omega\right) \quad \frac{1}{2}C_t^{GP}, \quad (13)$$

where the capacitance for the wire above ground C_t^{GP} is shown in Eq. (13), in which it may be more consistent (and slightly more accurate) to replace h by h_e. Since the air region typically dominates the admittance elements for a finitely conducting, but electrically dense conductive half space, these will also approximately hold for the finitely conducting half space.

Now inserting the complex permittivity the terminating admittance can be taken as

$$Y_t^{GP} = G_t^{GP} - i\omega C_t^{GP} \sim -i\omega\frac{2h4\pi\varepsilon_w}{\Omega^2}\left(1+4(1-\ln 2)/\Omega\right). \quad (14)$$

5. Comparison of full wave simulations with ATLOG for open and short circuit terminations without radiation

In this section we compare full wave simulations of transmission lines above a perfectly conducting ground using CST Microwave Studio software, with calculations using the transmission line model we refer to as ATLOG (Analytic Transmission Line Over Ground) [8].

All these comparisons are for the case of normal incidence and use a simple unit electric field amplitude sine-squared pulse of 200 ns duration. The simulations here provided have the following assumptions: the line has height h = 5 m, lengths L of 20 m and 40 m, and a radius of a = 1 cm (there is no insulation coating and the wire is a perfect conductor). Both cases with open circuits at both ends of the line, as well as cases with down conductors forming near short circuits at both ends of the line are considered here.

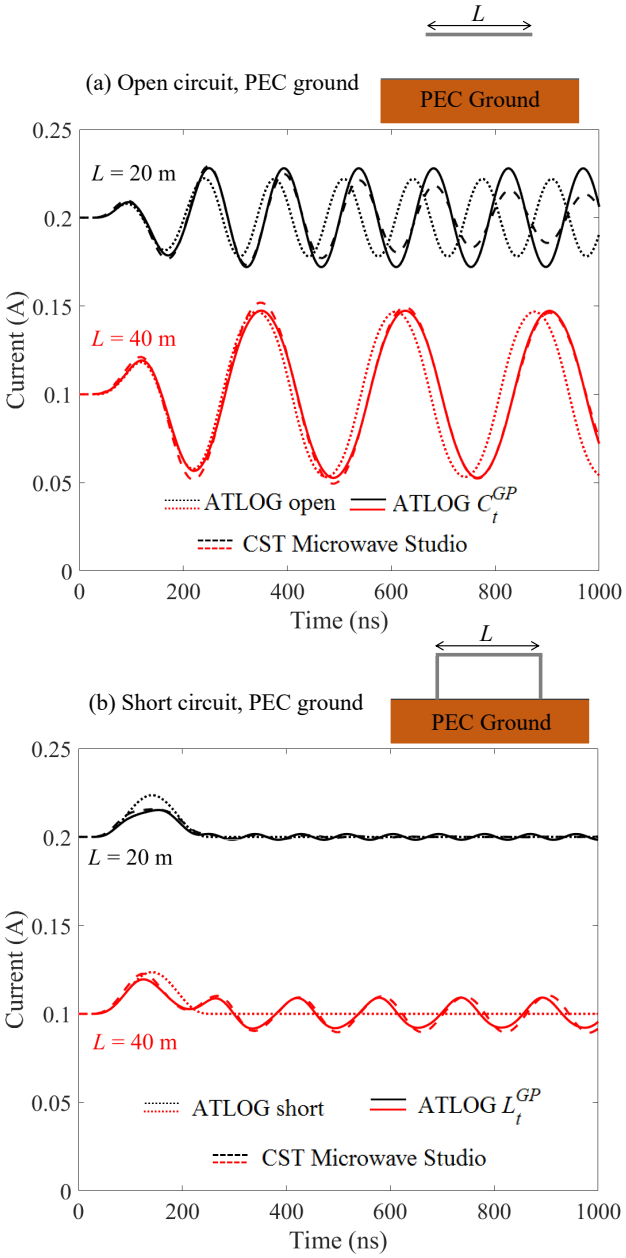

Figure 2: Comparison of full wave simulations (dashed curves) using CST Microwave Studio with transmission line having (a) idealized open circuits at each end (dotted curves) and terminating capacitors at each end (solid curves) and (b) idealized short circuits at each end (dotted curves) and terminating inductances at each end (solid curves). The line lengths are given on the left end of the graph, and an inset shows a schematic of the simulated geometry. Note that an arbitrary shift of +0.1 A has been added to the 40 m length result, and an arbitrary shift of +0.2 A has been added to the 20 m curve, to separate the different lengths and make the different curves readable.

The case with open circuits at both ends of the line is shown in Figure 2(a). The dotted curves have idealized open circuits at the ends of the transmission line, whereas the solid curves have the preceding terminating capacitive loads in (13). Notice that the phase shift caused by the terminating capacitive loads results in alignment of the curves in phase with the full wave simulations given by the

dashed curves. Radiation damping can be observed in the full wave simulations as illustrated by the slight decay shown in the dashed curve for the 20 m length.

The case with short circuits at both ends of the line is shown in Figure 2(b). The dotted curves have idealized short circuits at the ends of the transmission line, whereas the solid curves have the preceding terminating inductive loads in (9). Notice that the transmission line with idealized terminating short circuits shows no ringing and tracks the incident pulse used in these simulations. When the terminating inductances are added the response current rings due to the length of the line in agreement with the full wave simulations given by the dashed curves.

We sometimes run into a case where the port is formed at the base of the transmission line near the ground plane. In such a case the "open circuit" capacitive load is modified by the down conductor, and this analysis is reported in [14].

6. Ground rod termination

A ground rod termination into the conductive half space is often used in the "shorted" case. In other words, a series term must be added to the perfectly conducting ground plane termination impedance $Z_t^{GP} \to Z_t^{GP} + Z_r$. Three cases are illustrated in this section for the ground rod termination.

6.1. Low conductivity ground

If the ground conductivity is low, where the propagation decay length (or skin depth) is much larger than the ground rod length h_r, we regard this term as a series admittance (we are ignoring the inductance and resistance of the ground rod here) [2]

$$\frac{1}{Z_r} = Y_r = -i(\omega\varepsilon_4 \quad i\sigma_4)\frac{4\pi h_r}{\Omega_c}, \tag{15}$$

with $\Omega_c = \Omega_r - 2(1-\ln 2)$ and $\Omega_r = 2\ln(2h_r/a_r)$, where a_r is the ground rod radius.

6.2. High conductivity ground

In the case where the ground conductivity is high, such that the decay length is shorter than the ground rod length, we do not see the end of the ground rod, which is then treated as an antenna in the ground so that

$$Z_r = \frac{1}{Y_r} = Z_{04}\sqrt{\frac{Z_4}{Y_4}} = \sqrt{\frac{\omega\mu_0}{(\omega\varepsilon_4 + i\sigma_4)}}\frac{H_0^{(1)}(k_4 a_r)}{2\pi k_4 a_r H_1^{(1)}(k_4 a_r)}, \tag{16}$$

with $Z_4 \approx -i\omega\mu_0 h_r H_0^{(1)}(k_4 a_r)/\left[2\ k_4 a_r H_1^{(1)}(k_4 a_r)\right]$ and $Y_4 \approx -i2\pi(\omega\varepsilon_4 \quad i\sigma_4)k_4 a_r H_1^{(1)}(k_4 a_r)/H_0^{(1)}(k_4 a_r)$.

6.3. General conductivity ground: Transmission line model

If the ground rod is not electrically long or short we treat it using the preceding quasi-static results to obtain an end load in the transmission line model. Let us consider a transmission line with an end load Z_T. We then have

$$\frac{dV}{dz} = -Z_4 I, \quad \frac{dI}{dz} \quad Y_4 V, \tag{17}$$

or

$$\left(\frac{d^2}{dz^2} + k_4^2\right) I = 0, \tag{18}$$

with $k_4 = \sqrt{-Z_4 Y_4}$. We take $I = A\sin(k_4 z) + B\cos(k_4 z)$, for which $V = -k_4\left[A\sin(k_4 z) - B\cos(k_4 z)\right]/Y_4$, leading to

$$Z_T = \frac{V(h_r)}{I(h_r)} = \frac{k_4}{Y_4}\frac{A\sin(k_4 h_r) - B\cos(k_4 h_r)}{A\sin(k_4 h_r) + B\cos(k_4 h_r)}, \tag{19}$$

and

$$Z_r = \frac{V(0)}{I(0)} = -\frac{k_4}{Y_4}\frac{A}{B} = \frac{k_4}{Y_4}\frac{\sin(k_4 h_r) - \cos(k_4 h_r)Z_T Y_4/k_4}{\cos(k_4 h_r) + \sin(k_4 h_r)Z_T Y_4/k_4}. \tag{20}$$

The low frequency limit is $1/Z_r \sim h_r Y_4 + 1/Z_T$. The low frequency result for the electrically short ground rod in Eq. (15) can be written as

$$Y_h = G_h - i\omega C_h \sim \frac{2\pi h_r(\sigma_4 - i\omega\varepsilon_4)}{\ln(4h_r/a) - 1}. \tag{21}$$

If we impose the condition on this transmission line input impedance that it goes to the short limit $1/Z_r \to Y_h$ we have an end load

$$\frac{1}{Z_T} \to Y_h - h_r Y_4 \sim 2\pi h_r(\sigma_4 - i\omega\varepsilon_4)\left[\frac{1}{\ln(4h_r/a_r) - 1} - \frac{1}{\ln(4h_r/a_r) - 1 + 1 - \ln(2k_4 h_r) - \gamma}\right], \tag{22}$$

and

$$Z_T \sim \frac{\left[\ln(4h_r/a_r) - 1\right]\left[-\ln(k_4 a_r/2) - \gamma\right]}{2\pi h_r(\sigma_4 - i\omega\varepsilon_4)\left[1 - \ln(2k_4 h_r) - \gamma\right]}. \tag{23}$$

7. Radiation losses

Radiation losses are estimated by first finding the magnetic vector potential from the current distribution [27] and then integrating the Poynting vector over the sphere at infinity. For this evaluation we neglect the small loss part of the transmission line wavenumber and assume that $k_L \approx k$. We summarize the results for various end terminations [28] in this section.

7.1. Open-open case

This power radiated is

$$P = G_{rad}|V(0)|^2 = \frac{1}{2}G_{rad}|V(0)|^2 + \frac{1}{2}G_{rad}|V(\ell)|^2, \tag{24}$$

where for $k\ell \to n\pi$

$$G_{rad} = \frac{\omega\mu_0}{2\pi Z_c^2}kh_e^2 = \frac{\pi(kh_e)^2/\eta}{2\ln^2(2h_e/a)} = 2G_{rad}^{GP}, \tag{25}$$

with the characteristic impedance $Z_c = \eta/\pi \ln(2h_e/a) = 2Z_c^{GP}$ and $\eta = \sqrt{\mu_0/\varepsilon}$.

7.2. Short-short case

This power radiated is

$$P = R_{rad}|I(0)|^2 = \frac{1}{2}R_{rad}|I(0)|^2 + \frac{1}{2}R_{rad}|I(\ell)|^2, \quad (26)$$

where for $k\ell \to n\pi$

$$R_{rad} = \frac{\eta}{2\pi}(kh_e)^2 = 2R_{rad}^{GP}. \quad (27)$$

7.3. Open-short case

This power radiated is

$$P = \frac{1}{2}G_{rad}|V(0)|^2 + \frac{1}{2}R_{rad}|I(\ell)|^2, \quad (28)$$

and $G_{rad}Z_c^2 + R_{rad} = \eta(kh_e)^2/\pi = 2G_{rad}^{GP}Z_c^{GP2} + 2R_{rad}^{GP}$. We could place this perturbing radiation term exclusively at the shorted end, or exclusively at the open end, by setting the other term to zero. Note from the open-open and the short-short cases above we had

$$G_{rad}Z_c^2 = \eta(kh_e)^2/(2\pi) = R_{rad} = 2G_{rad}^{GP}Z_c^{GP2} = 2R_{rad}^{GP}, \quad (29)$$

which adds up to this same result, and hence it is better to add these radiation loads on each end of the open-short setup.

7.4. End reflection method

To treat radiation from longer lines ending in open circuits, particularly with large skin depths, it is more convenient to change to the description of a reflection from the line end by means of the Wiener-Hopf method as was done for the long antenna [29]. This was done both for the semi-infinite wire above a perfectly conducting ground in [15, 30, 31], which yields the same radiation result as obtained above in the open-open case in (25). The semi-infinite and finite wire above a finite conductivity ground was also analyzed in [32, 33].

8. Comparison of full wave simulations with ATLOG for open, short, and ground rod terminations including radiation

In this section we compare full wave simulations (using CST Microwave Studio software and/or EIGER) of transmission lines with various terminations to calculations using ATLOG when both terminating reactive loads in addition to radiation resistive loads are included.

All these comparisons are for the case of normal incidence and use a simple unit electric field amplitude sine-squared pulse of 200 ns duration. The simulations here provided have the following assumptions: the line has height h = 5 m, lengths L of 20 m and 40 m, and a radius of a = 1 cm (there is no insulation coating and the wire is a perfect conductor).

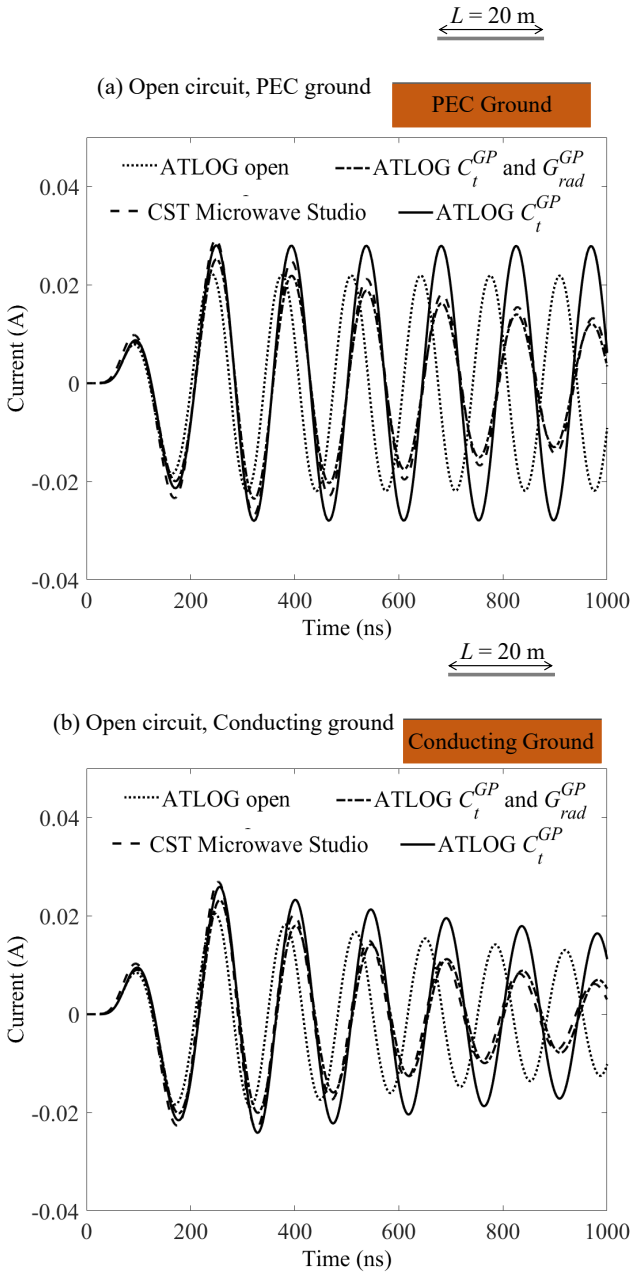

Figure 3: Comparison of full wave simulation (dashed curve) using CST Microwave Studio with the ATLOG transmission line calculations for a 20 m long section of line over (a) perfectly conducting ground and (b) a conducting ground with relative permittivity of 20 and conductivity of 0.01 S/m having open circuits at both ends. The dotted curve has idealized open circuits at each end, the solid curve has terminating capacitors at each end, and the dash-dot curve has terminating capacitors and radiation conductances at each end.

Simulations when the ends of a 20 m long section of line over perfectly conducting ground are open circuited are shown in Figure 3(a). The dashed curve is the full wave simulation, the dotted curve is ATLOG with idealized open circuits at the ends, the solid curve is ATLOG with capacitive loads at the ends, and the dash-dot curve is ATLOG with capacitive and radiation conductance loads at the ends of the line. Notice that the dash-dot and dashed

curves are showing reasonable agreement at the later times and are illustrating decay in amplitude due to radiation (there is no other loss in the problem being modeled).

Figure 3(b) shows a comparison of simulations when the ends of a 20 m long section of line over a conducting ground (with relative permittivity of 20 and conductivity of 0.01 S/m) are open circuited. Again, the dash-dot and dashed curves are showing reasonable agreement at the later times and are illustrating decay in amplitude due to radiation and ground losses.

Simulations when the ends of a 40 m long section of line over perfectly conducting ground are short circuited are shown in Figure 4(a). The dashed curve is the full wave simulation, the dotted curve is ATLOG with idealized short circuits at the ends, the solid curve is ATLOG with inductive loads at the ends, and the dash-dot curve is ATLOG with inductive and radiation resistance loads at the ends of the line. Notice that the dash-dot and dashed curves are showing reasonable agreement at the later times and are illustrating decay in amplitude due to radiation (there is no other loss in the problem being modeled).

Simulations when the ends of a 20 m long section of line over perfectly conducting ground are open circuited on the left and short circuited on the right are shown in Figure 4(b). The dashed curve is the full wave simulation, the dotted curve is ATLOG with idealized open and short circuits at the two ends, the solid curve is ATLOG with a capacitive load on the left end and an inductive load on the right end, and the dash-dot curve is ATLOG with capacitive-radiation conductance load on the left end and an inductive-radiation resistance load on the right end. Notice that the dotted curve is dominated by a single ringing frequency (phase shifted from the other curves) whereas the solid curve is exhibiting two ringing frequencies and phase alignment with the dashed and dash-dot curves. The radiation damping (proportional to the square of the wavenumber and line height) reduces the amplitude of the higher frequency and results in much better agreement between the ATLOG dash-dot curve and the full wave simulation.

Figure 5(a) shows a comparison of simulations when the ends of a 40 m long section of line over a conducting ground (with relative permittivity of 20 and conductivity of 0.01 S/m) are terminated with ground rods which are 1 m deep within the ground. The red dashed curve is the full wave simulation computed with CST Microwave Studio, while the dotted blue curve is the full wave simulation computed with EIGER. The dotted black curve is ATLOG with only the additional effect of the impedance of the ground rods, the dashed-dotted curve is ATLOG with idealized short circuits at the ends, the solid curve is ATLOG with inductive loads plus radiation resistance plus ground rods contributions at the ends. Notice that the solid, red dashed, and blue dotted curves are showing reasonable agreement at later times and are illustrating proper modeling with lumped loads.

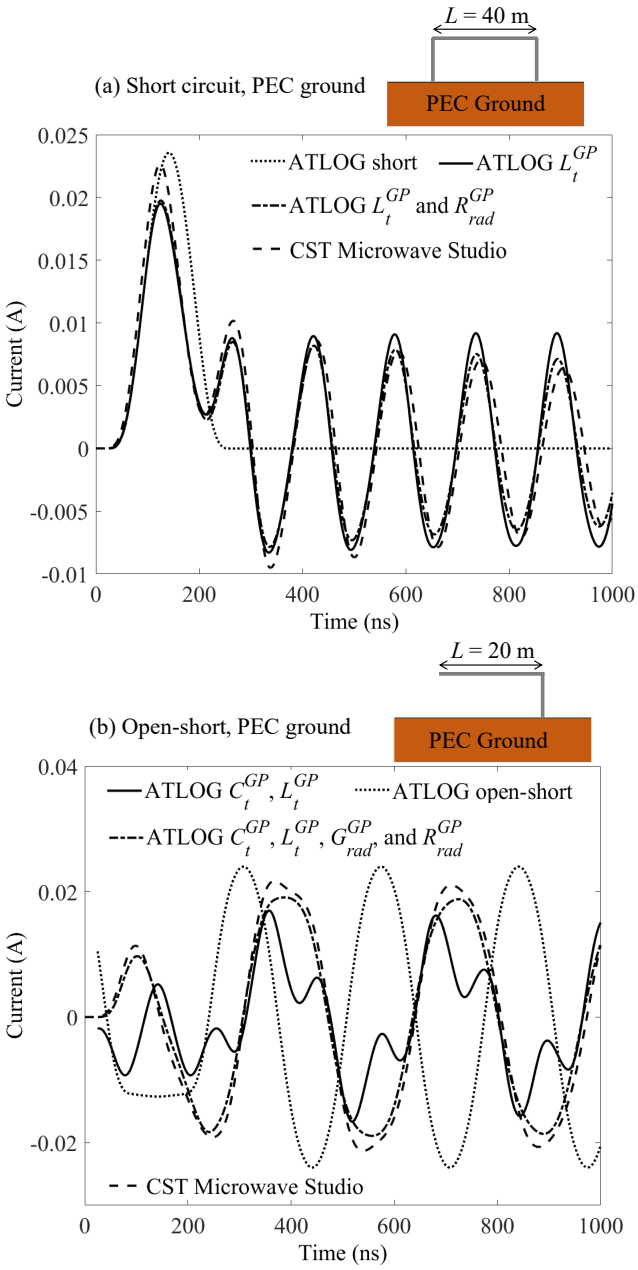

Figure 4: (a) Comparison of full wave simulation (dashed curve) using CST Microwave Studio with the ATLOG transmission line calculations for a 40 m long section of line over perfectly conducting ground having short circuits at both ends. The dotted curve has idealized short circuits at each end (and has no ringing at normal incidence), the solid curve has terminating inductors at each end and shows ringing, and the dash-dot curve has terminating inductors and radiation resistances at each end. (b) Comparison of full wave simulation (dashed curve) using CST Microwave Studio with the ATLOG transmission line calculations for a 20 m long section of line over perfectly conducting ground having an open circuit at the left end and a short circuit at the right end. The dotted curve has idealized open and short circuits at the two ends, the solid curve has a terminating capacitor and inductor at the respective ends, and the dash-dot curve has terminating capacitor-radiation conductance and inductor-radiation resistance at the respective ends.

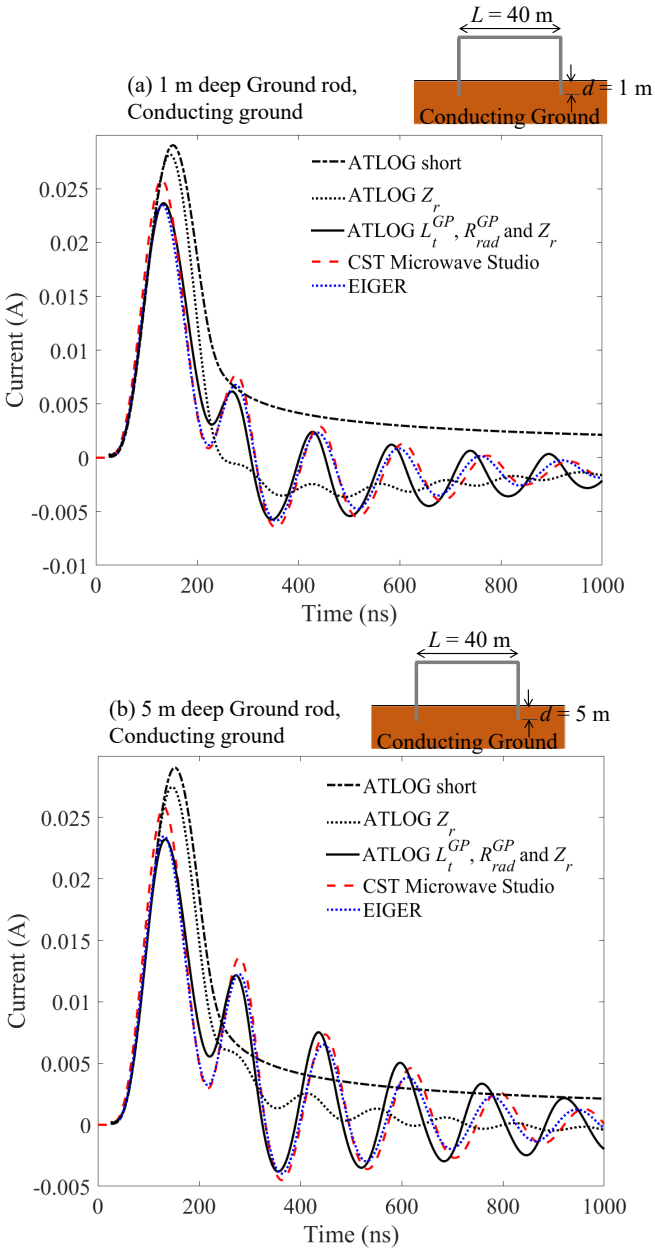

Figure 5: Comparison of full wave simulation using CST Microwave Studio (red dashed curve) and EIGER (blue dotted curve) with the ATLOG transmission line calculations for a 40 m long section of line over a conducting ground (with relative permittivity of 20 and conductivity of 0.01 S/m) having (a) 1 m deep and (b) 5 m deep ground rods at both ends. The dashed-dotted curve has idealized short circuits at each end, the black dotted curve has terminating rod impedances, and the solid curve has terminating inductors, rod impedance, and radiation resistances at each end.

Figure 5(b) shows a comparison of simulations when the ends of a 40 m long section of line over a conducting ground (with relative permittivity of 20 and conductivity of 0.01 S/m) are terminated with ground rods which are 5 m deep within the ground. Similar to the case in Figure 5(a), the solid, red dashed, and blue dotted curves are showing reasonable agreement at later times and are illustrating proper modeling with lumped loads.

9. Conclusions

In this paper, we constructed circuit models for the end loads used in a transmission line model of a wire above a conducting ground driven by an electromagnetic field. We considered the following terminations: open circuit, short circuit, and grounded rods. In the open case the effective capacitance (and conductance if the air is lossy) is estimated to represent the charge build up near the end of the line. In the shorted case the inductance, in addition to the ground rod impedance, are both estimated. The radiation damping is also discussed for various types of basic terminations. We compared the transmission line model here discussed to full wave simulations, and observed good agreement, validating the proposed lumped termination models. These analytical models allow to compute fast and reliable results and can be used in place of full-wave simulators, especially for long lines.

Acknowledgements

This work was supported by the Laboratory Directed Research and Development at Sandia National Laboratories. Sandia National Laboratories is a multimission laboratory managed and operated by National Technology and Engineering Solutions of Sandia, LLC, a wholly owned subsidiary of Honeywell International, Inc., for the U.S. Department of Energy's National Nuclear Security Administration under contract DE-NA-0003525. This paper describes objective technical results and analysis. Any subjective views or opinions that might be expressed in the paper do not necessarily represent the views of the U.S. Department of Energy or the United States Government.

References

[1] J. R. Carson, "Wave propagation in overhead wires with ground return," *The Bell System Technical Journal,* vol. 5, pp. 539-554, 1926.

[2] E. D. Sunde, *Earth Conduction Effects in Transmission Systems*. New York: Dover, 1967.

[3] J. R. Wait, "Theory of Wave Propagation Along a Thin Wire Parallel to An Interface," *Radio Science,* vol. 7, pp. 675-679, 1972.

[4] J. R. Wait, "Tutorial note on the general transmission line theory for a thin wire above the ground," *IEEE Transactions on Electromagnetic Compatibility,* vol. 33, pp. 65-67, 1991.

[5] R. G. Olsen, J. L. Young, and D. C. Chang, "Electromagnetic Wave Propagation on a Thin Wire Above Earth," *IEEE Transactions on Antennas and Propagation,* vol. 48, pp. 1413-1419, 2000.

[6] H. Kikuchi, "Wave propagation along an infinite wire above ground at high frequencies," *Proc. Electrotech. J.,* vol. 2, pp. 73-78, 1956.

[7] H. Kikuchi, "Wave propagation along an infinite wire above the ground in the high frequency region - on the transition from a ground return circuit to a surface waveguide," *Bull. Electrotech. Lab.,* vol. 1, pp. 49-61, 1957.

[8] S. Campione, L. K. Warne, L. I. Basilio, C. D. Turner, K. L. Cartwright, and K. C. Chen, "Electromagnetic pulse excitation of finite- and infinitely-long lossy conductors over a lossy ground plane," *Journal of Electromagnetic Waves and Applications,* vol. 31, pp. 209-224, 2017.

[9] L. K. Warne and K. C. Chen, "Long Line Coupling Models," *Sandia National Laboratories Report,* SAND2004-0872, Albuquerque, NM, 2004.
[10] D. Chang and J. Wait, "Extremely Low Frequency (ELF) Propagation Along a Horizontal Wire Located Above or Buried in the Earth," *IEEE Transactions on Communications,* vol. 22, pp. 421-427, 1974.
[11] E. F. Kuester, D. C. Chang, and S. W. Plate, "ELECTROMAGNETIC WAVE PROPAGATION ALONG HORIZONTAL WIRE SYSTEMS IN OR NEAR A LAYERED EARTH," *Electromagnetics,* vol. 1, pp. 243-265, 1981/01/01 1981.
[12] E. F. Kuester, D. C. Chang, and R. G. Olsen, "Modal theory of long horizontal wire structures above the earth: 1, Excitation," *Radio Science,* vol. 13, pp. 605-613, 1978.
[13] S. Campione, L. K. Warne, M. Halligan, O. Lavrova, and L. S. Martin, "Decay Length Estimation of Single-, Two-, and Three-Wire Systems Above Ground under HEMP Excitation " *Progress in Electromagnetics Research,* accepted, 2019.
[14] L. K. Warne and S. Campione, "Formulas for plane wave coupling to a transmission line above ground with terminating loads," *Sandia National Laboratories Report,* SAND2018-8736, Albuquerque, NM, 2018.
[15] R. W. P. King, *Transmission Line Theory*. New York: McGraw-Hill Book Co., 1955.
[16] D. R. Wilton, W. A. Johnson, R. E. Jorgenson, R. M. Sharpe, and J. B. Grant, "EIGER: A new generation of computational electromagnetics tools," *Sandia National Laboratories Report,* SAND96-0646C, Albuquerque, NM, 1996.
[17] R. M. Sharpe, J. B. Grant, N. J. Champagne, W. A. Johnson, R. E. Jorgenson, D. R. Wilton*, et al.*, "EIGER: Electromagnetic interactions GEneRalized," *Sandia National Laboratories Report,* SAND97-0576C, Albuquerque, NM, 1997.
[18] (2019). *CST Microwave Studio, https://www.cst.com/products/cstmws*.
[19] S. Ramo, J. R. Whinnery, and R. V. Duzer, *Fields and Waves in Communication Electronics*. New York, NY: John Wiley & Sons, Inc., 1965.
[20] E. F. Vance, *Coupling to shielded cables*: R.E. Krieger, 1987.
[21] K. S. H. Lee, *EMP Interaction: Principles, Techniques, and Reference Data*. Washington: Hemisphere Publishing Corp., 1986.
[22] F. M. Tesche, M. V. Ianoz, and T. Karlsson, *EMC Analysis Methods and Computational Models*. New York: John Wiley & Sons, Inc., 1997.
[23] K. C. Chen and L. K. Warne, "A uniformly valid loaded antenna theory," *IEEE Transactions on Antennas and Propagation,* vol. 40, pp. 1313-1323, 1992.
[24] L. K. Warne, W. A. Johnson, R. S. Coats, R. E. Jorgenson, and G. A. Hebner, "Model For Resonant Plasma Probe," *Sandia National Laboratories Report,* SAND2007-2513, Albuquerque, NM, 2007.
[25] F. W. Grover, *Inductance Calculations*. New York: Dover Pub., Inc., 1946.
[26] S. A. Schelkunoff, *Advanced Antenna Theory*. New York: John Wiley & Sons, Inc., 1952.
[27] E. C. Jordan and K. G. Balmain, *Electromagnetic Waves and Radiating Systems*: Prentice-Hall, 1968.
[28] R. W. P. King and J. C.W. Harrison, *Antennas and Waves*. Cambridge, MA: MIT PR., 1969.
[29] L. Shen, T. Wu, and R. King, "A simple formula of current in dipole antennas," *IEEE Transactions on Antennas and Propagation,* vol. 16, pp. 542-547, 1968.
[30] S. Tkachenko and J. Nitsch, "Investigation Of High-Frequency Coupling With Uniform And Non-Uniform Lines: Comparison Of Exact Analytical Results With Those Of Different Approximations," presented at the Proc. Int. Union. Radio Science XXVII General Assembly, Maastricht, The Netherlands, 2002.
[31] L. A. Vaynshteyn, *The Theory of Diffraction and the Factorization Method*. Boulder, CO: The Golem Press, 1969.
[32] R. G. Olsen and D. C. Chang, "Analysis of semi-infinite and finite thin-wire antennas above a dissipative earth," *Radio Science,* vol. 11, pp. 867-874, 1976.
[33] R. G. Olsen and D. C. Chang, "Electromagnetic Characteristics Of A Horizontal Wire Above A Dissipative Earth - Part III: Analysis Of Semi-Infinite And Finite-Thin Wire Antennas," *Scientific Report No. 6, Electromagnetics Laboratory, Dept. of Electrical Engineering, U. of Colorado, Boulder, CO,,* 1974.